

Copyright (to be inserted by the publisher)

Uses of Hyperspectral and Multispectral Laser Induced Fluorescence Imaging Techniques for Food Safety Inspection

Moon S. Kim¹, Alan M. Lefcourt¹, Yud-Ren Chen¹ and Sukwon Kang²

¹ Instrumentation and Sensing Laboratory, Animal and Natural Resources Institute
USDA Agricultural Research Service, Powder Mill Rd. Bldg 303, BARC-East
Beltsville, MD 20705, U.S.A.
kimm@ba.ars.usda.gov

² National Agricultural Mechanization Research Institute, Rural Development Administration
249 Seodun-don, Gwonson gu, Suwon, Gyeonggi-do, Korea

Keywords: Hyperspectral imaging, multispectral imaging, fluorescence, laser-induced fluorescence, animal fecal contamination, food safety.

Abstract. Spectral imaging including machine vision and multispectral imaging can provide a rapid, nondestructive means to assess agricultural commodities for their quality and safety for human consumption. These nondestructive techniques generally rely on reflectance measurements; the most commonly used spectral regions range through the visible (Vis) to the near infrared (NIR). Another optical sensing technique is based on fluorescence that is generally regarded as more sensitive optical sensing tools compared to reflectance techniques. Recently, we developed two imaging systems for food safety research; a laboratory-based hyperspectral imaging system capable of both reflectance and fluorescence measurements and a multispectral laser induced fluorescence imaging system. Because many contiguous spectral bands are acquired with each hyperspectral image pixel, the resulting data quantity makes uses of hyperspectral imaging spectrometer for on-line food safety inspection impractical. Instead, the spectral and spatial information is used to determine several optimal wavebands that can be implemented to a multispectral imaging system. We present a systematic method for using hyperspectral image data to identify few wavebands to be used in multispectral detection systems. Also presented is a two-band ratio as a multispectral fusion method along with automated detection for animal feces contamination on apples. The fluorescence imaging techniques demonstrated that even minute animal feces, not clearly visible to human eye, could be detected. Practical considerations for development of multispectral fluorescence imaging systems for on-line uses are also discussed.

Introduction

Numerous people are affected by foodborne illness each year and safe production of food commodities is of public concern. Researchers at the Instrumentation and Sensing Laboratory (ISL), Agricultural Research Services (ARS), United States Department of Agriculture (USDA) in Beltsville, Maryland, have been working on a postharvest food safety project entitled "Development of Technology for Automated On-Line Inspection of Animal Carcasses and Plant Produce." The research effort is essentially a response to the needs of the regulatory government agencies, Food Safety and Inspection Service (FSIS/USDA) and the Food and Drug Administration (FDA), and the emerging needs of industry under the HACCP (Hazards and Critical Control Points) and HIMP (HACCP-based Inspections Models Project) activities. Our primary responsibilities have been to develop new methodologies, instruments and on-line inspection strategies that will improve the nation's ability to inspect and classify chicken carcasses objectively, and provide a nondestructive means for detecting defective and animal feces contaminated fruits and vegetables. The results of our research efforts have regulatory, industry, and research uses.

Spectral imaging techniques typically utilizing reflectance in the visible (Vis) to near-infrared (NIR) allow rapid nondestructive detection/inspection of anomalies present in food commodities [1,

2]. Another sensing technique available in these spectral regions is fluorescence. A number of biological compounds emit fluorescence in the Vis to far-red region of the spectrum when excited with ultraviolet (UV) radiation [3, 4]. Fluorescence techniques are generally regarded as a more sensitive optical tool when compared to reflectance. Several fluorescence imaging platforms developed in our laboratory for uses in food safety research include a scanning hyperspectral imaging spectrometer [5] and laser-induced fluorescence (LIF) imaging systems with multispectral capabilities [6].

Animal fecal matter is the primary source of pathogenic bacteria on meat and in unpasteurized juices [7, 8]. Current government regulations stipulate no-visual evidence of fecal matter on meats or on fruits used to make juices [9, 10]. The route of contamination of apples with animal feces includes air-borne transport dust from near-by pastures or by direct contact with animal droppings [7]. The versatile uses of the fluorescence imaging techniques for postharvest food safety inspection are demonstrated using apples empirically contaminated with a range of diluted animal feces spanning from visible to invisible to human eye. The paper describes methodologies for identifying few optimal spectral bands with the use of hyperspectral imagery principal component analysis and demonstrates a simple multispectral fusion technique for automated detection of fecal contamination on apples. Also discussed are considerations for the development of multispectral laser induced fluorescence (LIF)-based imaging systems with potentials for rapid on-line applications at food processing plants.

Materials and Methods

Apples. Apples, cultivars 'Golden Delicious', were "tree run" (no coating of wax or fungicide) and were acquired from Rice Fruit Company (PA, USA). The samples were transported to the ISL and stored in a cold room (3° C). Apples, even individual apples, displayed color variations that may have resulted from differential environmental growth conditions causing variations in pigmentation and ripeness. A total of 96 apples without any physical defects (that were visually identifiable) were randomly selected for imaging study. Hence, normal apples (uncontaminated) constituted a range of the natural skin color variations.

Feces Samples and Application. Fresh cow feces from animals fed feedstuffs containing green roughage were collected from USDA farm facilities in Beltsville, MD. Feces contaminated spots on apples were created by applying cow feces diluted with distilled H₂O (three concentrations, 1:2, 1:20 and 1:200 by weight). Using a pipette, 30 µl of each dilution of cow feces was applied to sides of individual apples starting 1:2 on one of the quadrants, followed by 1:20 and 1:200 dilutions, respectively, on the adjacent quadrants in clockwise direction. Note that 1:200 feces dilution spots on apples were not visible and 1:20 treatments resulted transparent contamination spots on apples (not easily discernable visually).

Hyperspectral Imaging System. Hyperspectral imaging data consist of a volume of spatial and contiguous spectral information. The ISL hyperspectral imaging system is a line-by-line scanning imaging spectrometer with spectral range in the VIS to NIR from 425.7 nm to 951.2 nm. The system was designed to capture reflectance and steady-state fluorescence measurements from samples up to 30 cm wide. The hyperspectral imaging system consists of a 16-bit digital imager, a spectrograph, and a lens along with a sample transport mechanism and lighting sources (Fig. 1). The digital imager contains a thermo-electrically cooled (three-stage Peltier device), electron multiplying charge-coupled device (EMCCD) with 288 (V) X 560 (H) pixels (Andor Inc., MA, USA). The line scan spectrograph (ImSpector-V9, Spectral Imaging LTD., Finland) is based on prism-grating-prism (PGP) optics and has spectral resolution of approximately 10 nm full width at half maximum (FWHM). The spectrograph coupled to an f 1.4 C-mount lens (Schneider Optics Inc., NY) disperses incoming radiation along the each spatial location on the scan line into spectral dimension. Note that not all EMCCD pixels were used for hyperspectral imaging. The system typically captures 460 spatial pixels while 2× vertical pixel binning is used for the spectral dimension. Effective spectral regions for fluorescence were determined to be from 425 to 772 nm

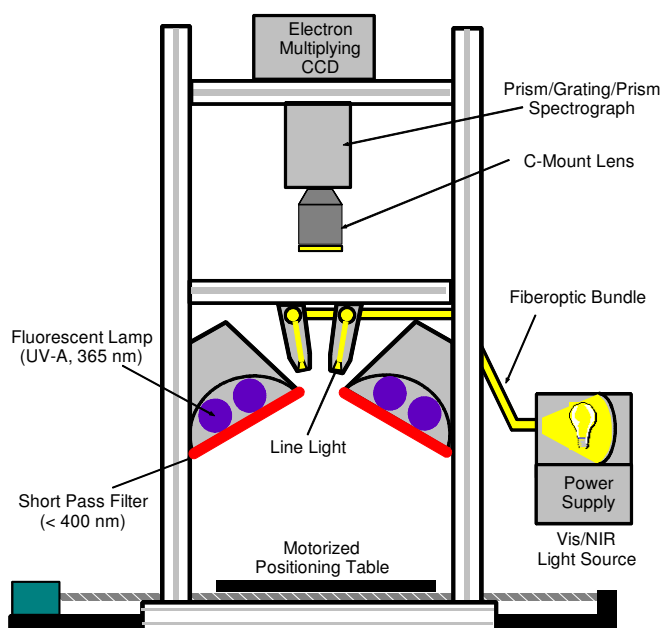


Fig. 1. Schematic diagram of the hyperspectral imaging system.

lighting, two continuous wave (CW), UV-A fluorescent lamp assemblies (Model XX-15A 365 nm, Spectronics Corp., NY, USA) are arranged toward the line of field of view (FOV) at 30° backward and forward. Short-pass filters (UG1, Schott Glass Co. PA, USA) are placed in front of the lamp housing to prevent transmittance of radiations greater than approximately 400 nm.

Data corrections were performed on raw image data to obtain flat-field corrected fluorescence measurements. Individual pixel responses obtained from flat-field fluorescent targets were normalized to the average of all the flat-field pixel intensities to correct for heterogeneous responses of the system. A detailed description of spatial calibration procedures and instrument peripherals for reflectance imaging are omitted for brevity (see Kim et al., 2001 [5]).

Data Acquisition and Image Processing. Interface software (MS VisualBasic, Version 6.0) operating in MS Windows environment was developed to control the EMCCD camera system and acquire image data. Individual line scan image data were saved in a 16 bit binary format along with a header file (per set) containing imaging parameter information. We also developed image process/analysis software to perform dark current subtraction and flat field-spatial corrections, and then to merge individual line scan image data to a volume of band sequential hyperspectral image data format comparable to commercial software packages such as ENVI (Environment for Visualizing Images, Research Systems, Inc., Colorado, USA). In addition, the following functions were incorporated in the software: image visualization/enhancement, descriptive statistics of a rectangular region of interest (ROI), simple and automated histogram-threshold classifications, arithmetic operations (i.e., band ratio), spatial pixel binning, spectral and spatial data retrieval, image transformations (e.g., convolution and morphological filters), and merging sets of hyperspectral image data files (or ROI) to a single file.

Methods. Hyperspectral imaging encompasses the features of imaging and spectroscopy, (i.e., spatial and spectral information). A contiguous spectrum associated with each spatial location in an image equates to a large volume of data. There may also exist redundancy in spectral information. The large volume of data also limits the on-line use of hyperspectral imaging techniques at food processing plants when considering the speed requirements for real-time processing. The major goal for the use of hyperspectral imagery was to determine few spectral bands and image processing algorithms, keeping the algorithms simple for real-time image analyses, that allow fecal-contaminated surfaces to be differentiated from uncontaminated apple surfaces. The selected wavelengths can be used in multispectral imaging systems that are more suitable for on-line

(spectral range where fluorescence emission occurs with UV-A excitation). This results 79 spectral channels for fluorescence imaging with approximately 4.5 nm channel interval.

A programmable, precision positioning table (Velmex Inc., Bloomfield, NY, USA) moves samples transversely through the line of the FOV (field of view). The use of programmable positioning table allows geospatially identical sample images for fluorescence and reflectance measurements acquired independently. A total of 8 sets of hyperspectral image data, 12 apples per set arranged 2 rows by 6 columns on the positioning table, were acquired for this investigation. For each line scan, the positioning table was incremented by 1 mm and 600 mm per set of apples were required.

Two independent light sources provide sample illumination for fluorescence and reflectance, respectively. For fluorescence

applications at processing plants.

Two approaches were used to evaluate the voluminous hyperspectral fluorescence images of feces contaminated apples. First, spectral bands for analyses were initially selected based on the emission maxima of apples and feces at approximately 460, 550, 670, and 685 nm [11]. These individual fluorescence bands were evaluated to study the effects of spatial intensity variations across the contaminated and normal apple surfaces. Second, hyperspectral image data with entire spectrum regions (79 channels) were subjected to principal component analysis (PCA) using ENVI software. Note that PCA was performed on a hyperspectral image data containing all 96 apples (8 sets of files merged). Images shown in this paper are ROI of 9 apples, linearly stretched gray-scale in standard 8-bit bitmap format.

Subsequently, individual principal component (PC) score images were visually evaluated to determine those PC images showing 1) all three feces contamination spots on individual apples, and 2) contrasting score values (gray levels) between the feces contamination spots and apple surfaces for potential discrimination of the two classes. Each PC image is a linear sum of images at individual wavelengths weighted by corresponding spectral weighing coefficients (eigenvectors). The wavelengths where weighing coefficients at local maximum and minimum with large absolute coefficient values indicate the dominant spectral regions. Additional transformations tested to discriminate fecal-contamination over the range of normal apple surfaces were two band ratio images using the dominant wavelengths found by the PCA. Individual ratio images were subjected to a nonparametric and unsupervised, histogram threshold method by Otsu (1979 [12]) to test automated detection of feces contamination on apples. To allow analyses of only the areas of apple surfaces, mask image was created using a simple threshold applied to green band images.

Results and Discussion

Hyperspectral Fluorescence Imagery. Fig. 2 shows gray-scale fluorescence images of feces contaminated Golden Delicious apples at 460 (F460), 550 (F550), 670 (F670), and 685 nm (F685), respectively, obtained by the hyperspectral imaging system. F460 and F550 represents emission

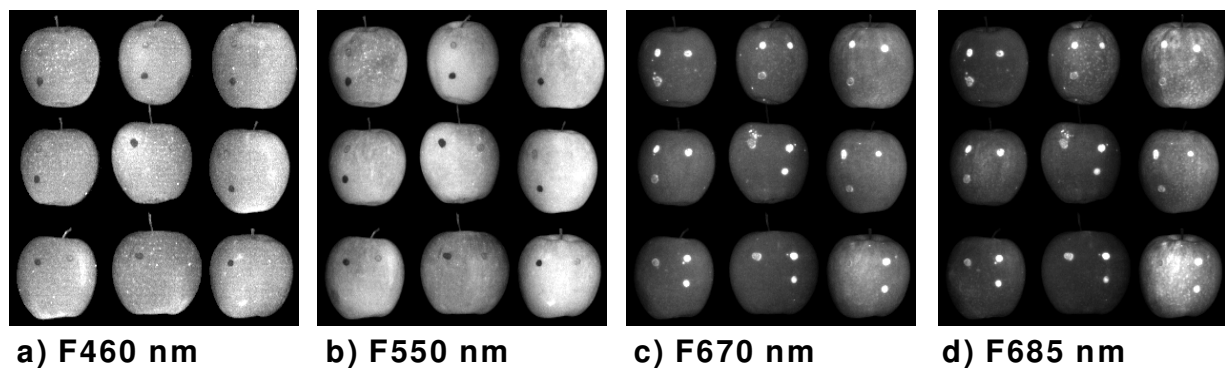


Fig. 2. Fluorescence images at 460, 550, 670, and 685 nm acquired with the ISL hyperspectral imaging system. The image histograms were linearly stretched to show visual contrast between the feces contamination spots and apple surfaces.

peak regions in the blue-green region of the spectrum and a myriad of plant compounds are responsible for the broad emissions [3, 4]. The images at F670 and F685 represent emission peak regions (due to chlorophyll *a* and its metabolites) for animal feces and apples, respectively [11]. The difference in the peak wavelengths may arise due to the state the compounds exist (i.e., unbound in feces vs. protein bound in intact plants as well as solvent effect). F460 and F550 exhibited similarities in fluorescence responses in that 1:2 feces treatments are clearly visible as darker spots compared to apple surfaces. In contrast, the F670 and F685 responses are markedly

different from the F450 and F550 suggesting that compounds other than chlorophyll *a* are responsible for the blue-green emissions.

The relative fluorescence intensities (RFI) for feces contaminated spots are generally higher compared to apple surfaces at F670 and F685, except the upper right and lower right greener apples in Fig. 2c and 2d. Note that these greener apple surfaces at F670 (emission maximum for animal feces) exhibit less RFI variation compared to F685. The F670 and F685 images reveal most of 1:20 and 1:200 feces contamination spots, which are not readily visible to human eye, with high (bright) fluorescence responses. These spots also exhibit higher fluorescence compared to the 1:2 spots. This observation is attributed to the additive effect of the transparent feces cover on fluorescent apple backgrounds and the effect of a strong self-absorption for higher 1:2 feces concentration [6].

The apples not clear showing the 1:2 feces contamination spots at F670 and F685 are the greener apples that have relatively higher chlorophyll *a* contents. However, these 1:2 spots are readily discernable at F450 and F550. In general, because of the heterogeneous fluorescence responses from uncontaminated apple surfaces and the variability in fluorescence responses of feces relative to the concentration of the applied feces, a single (monochromatic) waveband image may not allow for reliable detection of fecal contamination. However, the observations suggest that a fusion of multispectral fluorescence images in the blue-green to red regions of the spectrum may provide a sensitive basis for detection of fecal contamination regardless of the variations in apple coloration and feces concentration.

Principal Component Analysis and Wavelength Selection. Fig. 3 illustrates the first to the eighth principal component (PC-1 to PC-8) score images obtained by PCA of hyperspectral fluorescence images of fecal contaminated Golden Delicious apples. The PC-1 image represents a composite of transformed information from all the spectral regions, which accounts for the largest variance. Subsequent PC images are ordered in terms of the sample variance size; PC-1 to PC-8 accounted for 99.89 % of the variance, thus PCA can also be used as a means for dimensionality reduction of higher feature space data.

Individual PC images exhibit unique features based on spectral variation of the image data. Prominent features observed in these images are the apple color variation and feces contamination on apples (and some minor system aberrations, typically at higher PCs). The PC-2, 5 and 6 images show all three (1:2, 1:20, and 1:200 dilution) feces contamination spots on individual apples. PC-2 shows feces contamination areas as darker spots compared to surround apple surfaces and opposite trends in gray-scale colors (i.e., white spots for feces) were observed in PC-5 and PC-6. This observation suggests that the contrasts (in PC score values) between feces contamination spots and apple surfaces provide potential for classification or discrimination of two classes, regardless of the concentrations of feces and the variations in apple colors (within and between apples).

Fig. 4 illustrates spectral weighing coefficients (eigenvectors) for the PC-2, PC-5, and PC-6 images and the dominant wavelengths depicted as local minimum and maximum. The wavelengths were identified to be 534 and 681 nm for PC-2; 481, 556, and 663 nm for PC-5; and 534, 609, 663, 681, and 722 nm for PC-6. The dominant wavelengths by the selected individual PCs shared few common wavelengths as well as slightly blue or red-shifted wavelengths from the naturally occurring emission peak wavelengths. Blue-green emissions from the samples with UV excitation are convoluted emissions from a mixture of many compounds where individual compounds exhibit broad emission characteristics with varying wavelength peak locations in nature. In general, the selected dominant wavelengths nearly coincided with the fluorescence emission maxima observed from the sample materials. Hence, a slight difference in the peak wavelength locations (or center wavelengths) in the broad blue-green emission bands may have no significant, especially for choosing filters for multispectral imaging applications.

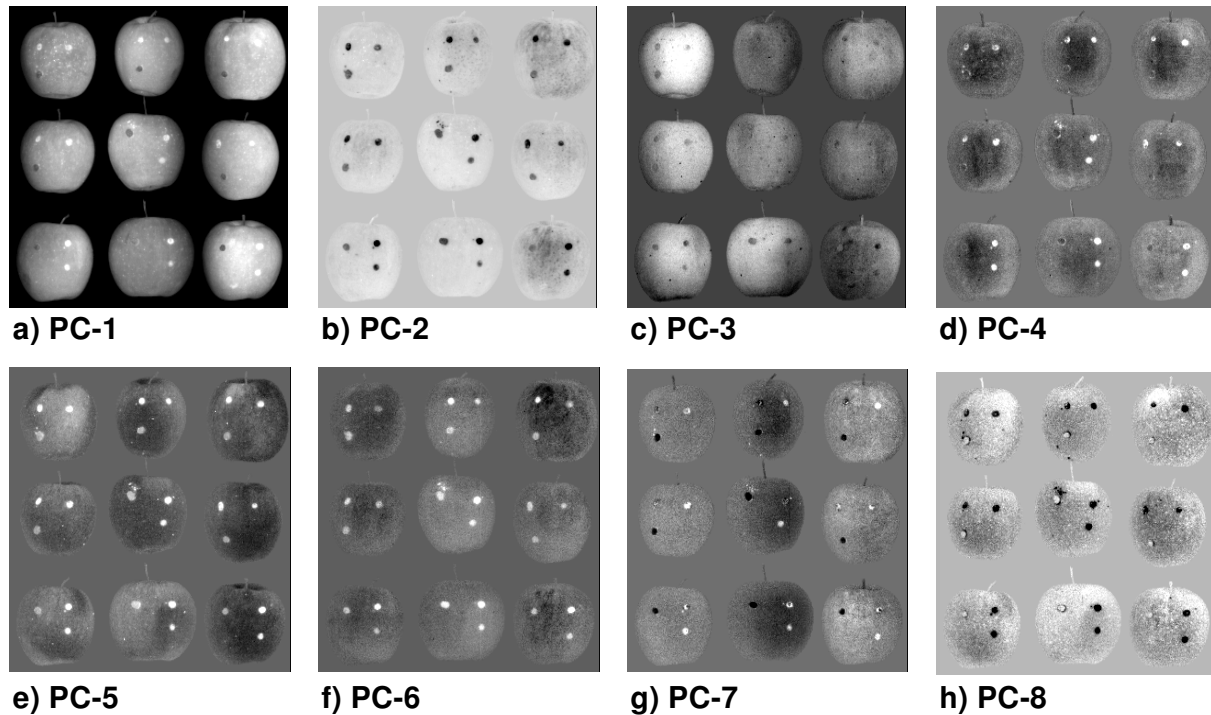


Fig. 3. First to eighth principal component (score) images obtained from the PCA of hyperspectral fluorescence images of feces contaminated Golden Delicious Apples. These PC images accounted for 99.89 % of the variance.

However, fluorescence emission peak in the red for animal feces occurs at approximately 670 nm, specifically due to chlorophyll *a* and its byproducts, and it exhibits relatively narrower spectral characteristics compared to the blue-green emissions. The PC-method indicated slightly blue-shifted peak wavelength at 663 nm. As observed in the individual peak bands, the heterogeneity in RFI for apple surfaces was less at 670 nm compared to 685 nm, and further blue-shifted wavelength at 663 nm may even further reduce the effect of heterogeneous responses from for apple surfaces with variegated chlorophyll *a* contents or colorations. The secondary minor peaks (spill-over) from chlorophyll *a* and its byproducts are typically observed in the far-red region from 705 to 735 nm. In addition, the 609 nm region is where a transition from blue-green to red emissions occurs with relatively low fluorescence emission. Note that the higher the PC is, the more complex the spectral weighing coefficients are in terms of dominant wavelengths. Thus, it becomes more difficult to understand the underlying fundamentals in spectral contributions to the construction of PC images.

The PC images were constructed based on a linear combination (sum) of the original data weighted by corresponding weighing coefficients. The PC-2, PC-5, and PC-6 images

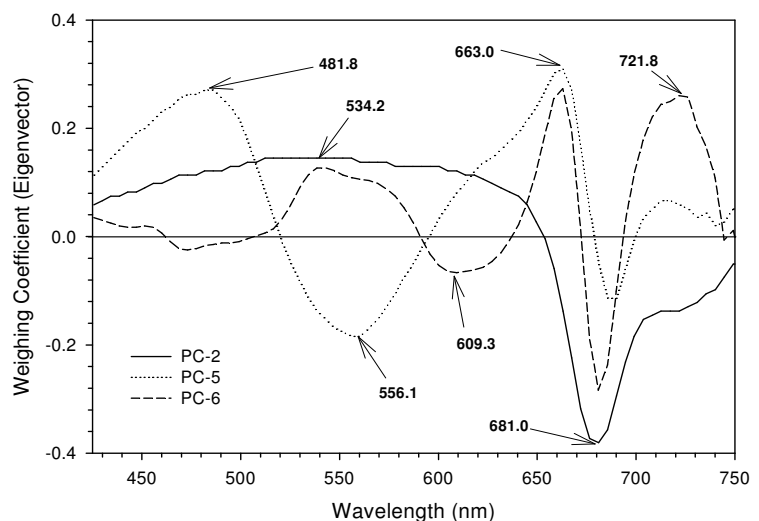


Fig. 4. Spectral weighing coefficients (eigenvectors) for PC-2, PC-5 and PC-6 obtained from the PCA of hyperspectral fluorescence images of Golden Delicious Apples treated with diluted cow feces.

can be approximated by linearly combining the original images at the selected dominant wavelengths [13]. For the PC-2 image, with the use of two dominant wavelength regions, a broad band in the blue-green and red region centered at 681 nm, the darker feces contamination spots and lighter apple surfaces were the result of subtracting the red region from the blue-green regions weighted by weighing coefficients. Another simple multispectral fusion method that may amplify the feature differences is ratio of the two spectral band regions.

Two band simple ratio images using all pair combinations of the PCA-selected wavelengths were created. Fig. 5a illustrates the ratio image of F663/F556 that yielded a minimal number of false positive pixels for feces contamination spots. The histogram of the ratio image shows that the ratio resulted a normal distribution for apple surfaces (Fig. 5b). It also shows the resultant threshold value (1.627) determined by the Otsu method. Binary image (automated detection results) created using the threshold value is shown in Fig. 5c. Note that all the ratio images were subjected to the unbiased automated threshold method to determine the best ratio combination. In general, ratio of F663 to either of the selected blue-green or F609 band resulted in similar automated detection results with minimal false positives (figure was omitted for brevity). A cluster of false positives with very few pixels seen in the middle apple near the 1:20 feces spots can be removed by using a spatial filter. Some area in the same apple above the 1:2 feces spot is actual feces contamination as splatter or smear occurs when applying feces dilution on apples.

Considerations for Development of Multispectral Imaging Systems. Common components of fluorescence sensing systems include a high intensity, monochromatic light as the excitation source, and a photon detection device. Typically, a CW light source is very stable and thus can provide constant excitation energy for steady-state fluorescence. However, due to low quantum yields from biological samples, systems using a CW light source require a dark environment for detection of fluorescence. Lasers are capable of emitting coherent light with a high degree of monochromaticity and provide an ideal excitation light for fluorescence (thus, called Laser-Induced Fluorescence). Pulsed lasers have the advantage of having high energy with a short pulse duration less than 10 ns, which results in time-dependent fluorescence emissions in ns time scale. A fast-gated detection system synchronized to laser pulses can capture a fluorescence emission before it

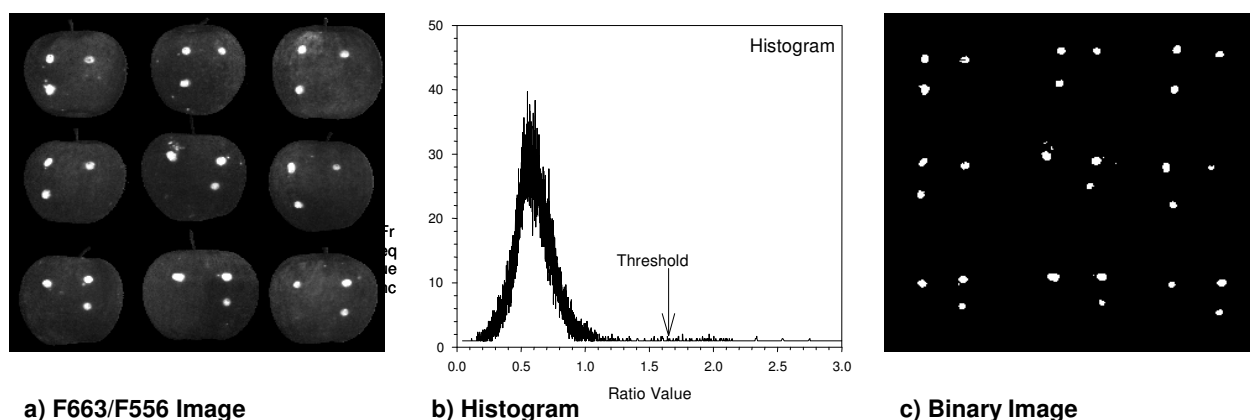


Fig. 5. a) Fluorescence ratio image (F663/F556) of Golden Delicious apples contaminated with diluted cow feces. b) F663/F556 image histogram and the threshold value determined by the automated histogram threshold method. c) Resultant binary image of automated histogram-threshold method for feces contamination spots on apples.

decays; the intensity of ambient light is several orders of magnitude lower than that of the fluorescence emissions at ns scale and, thus, can effectively be ignored. The rapid measurement time allow use of LIF techniques for non-stationary targets in ambient light. Pulse lasers typically emit beam of light with small foot print size. Alternatively, a pulse laser beam with sufficient power can be expanded with the use of lens so as to stimulate measurable fluorescence emissions from

large samples, and a readily available intensified-gated CCD detector can be used for imaging applications. This allows expansion of point source measurements to imaging applications for spatial analysis.

Multispectral imaging can be achieved either by acquiring individual band responses sequentially using a filter wheel or several spectral bands simultaneously using a common aperture device. Sequential imaging with the use of a filter wheel reduces the maximum potential imaging rate due to time lapses between acquisitions of individual spectral bands and, thus, is not appropriate for moving targets or when rapid acquisition of multispectral data are needed. Several types of common aperture devices are readily available that allow multispectral (two-to-four spectral bands) imaging of samples with a single image acquisition. There are some practical considerations for choosing the filters used in the multispectral adapter. In order to optimize the useful dynamic response ranges of the imaging system, two wavelength dependent factors need to be considered: the quantum efficiency of the imaging system and the relative signal intensity from the samples. With the use of representative sample materials, the FWHM of individual band pass filters near the center of the selected wavelength can be chosen so that the signal throughputs for individual wavelengths are similar.

The advent of new sensor technologies and peripherals make the on-line use of fluorescence techniques feasible. We developed such a common aperture multispectral laser induced fluorescence imaging system rapidly capture fluorescence images from a relative large object in ambient light [6]. With an expanded, frequency tripled Nd:YAG laser beam (355 nm) as the excitation source, fluorescence images at a multiple spectral bands are simultaneously captured from a target area up to 30 cm in diameter. We demonstrated the potential utilities of multispectral LIF imaging for food safety inspection [6, 14].

Summary

Hyperspectral imaging-PCA was used to determine several wavelengths that allow classification or discrimination of feces contaminations on Golden Delicious apples. Ratio image of the two selected wavelength bands by the PCA method at 556 and 663 nm provided automated detection of a range of diluted feces contamination spots on apples with a minimal of false-positives regardless apple surface color variations. The investigation demonstrated that fluorescence imaging techniques is a sensitive optical method in that diluted feces contamination spots not visible to human eye can be detected. Practical considerations for development of multispectral fluorescence imaging for on-line uses are also discussed.

References

- [1] B. Park, Y. R. Chen Y.R. and M. Nguyen: J. Agri. Eng. Res. Vol. 69 (1998), p. 351.
- [2] K. Chao, B. Park, Y.R. Chen, W.R. Hruschka, and F.W. Wheaton: Appl. Eng. in Agri. Vol. 16 (2002), p. 581.
- [3] E.W. Chappelle, J. E. McMurtrey, and M.S. Kim: Remote Sens. Environ. Vol. 36 (1991), p. 213.
- [4] M. Lang, F. Stober, and H.K. Lichtenthaler: Radiant Environ. Biophys. Vol. 30 (1991), p. 333.
- [5] M.S. Kim, Y.R. Chen, and P.M. Mehl: Trans. of ASAE Vol.44 (2001), p. 721.
- [6] M.S. Kim, A.M. Lefcourt, and Y.R. Chen: Applied Optics, Vol. 42 (2003), p. 3927.
- [7] P.S. Mead, L. Slutsker, V. Dietz, L.F. McCaig, J.S. Bresee, C. Shapiro, P.M. Griffin, and R.V. Tauxe, Emerging Infectious Diseases Vol. 5 (1999), p. 607.

This list of references is to be included by the publisher.

- [8] S.H. Cody, M.K. Glynn, J.A. Farrar, K.L. Cairns, P.M. Griffin, J. Kobayashi, M. Fyfe, R. Hoffman, A.S. King, J.H. Lewis, B. Swaminathan, R.G. Bryant, and D.J. Vugia: *Annl. Int. Med.* Vol. 130 (1999), p. 202.
- [9] Food Safety Inspection Service: FSIS Directive 6420.1 (1998), p. 1.
- [10] Food and Drug Administration (FDA): *Federal Registry* 66(13) (2001), p. 6137.
- [11] M.S. Kim, A.M. Lefcourt, and Y. R. Chen: *J. Food Prot.* Vol. 66(7) (2003), p. 1098.
- [12] N. Otsu: *Man, and Cybernetics* Vol. SMC-9(1) (1979), p. 62.
- [13] M.S. Kim, A.M. Lefcourt, K. Chao, Y.R. Chen, and I. Kim: *Trans. of ASAE* Vol. 45 (2002), p. 2027.
- [14] A.M. Lefcourt, M.S. Kim, and Y.R. Chen: *Applied Optics*, Vol. 42 (2003), p. 3935.